3-Dimensional Monte Carlo Simulations of Directional Precipitate Coarsening in Alloys under External Load

Himadri Gupta*, Richard Weinkamer**, Peter Fratzl***, and Joel L. Lebowitz*

*Departments of Mathematics and Physics, Rutgers University, Busch Campus, New Brunswick, 08903 New Jersey, USA. **Institute of Materials Physics, University of Vienna, Strudlhofgasse 4, A-1090 Wien, ***Erich Schmid Institute of Materials Science, Austrian Academy of Sciences, and University of Leoben, Jahnstrasse 12, A-8700 Leoben, Austria

Keywords: phase separation, elastic interaction, Monte Carlo simulation, misfit, external stress, directional coarsening, rafting, structure function, microstructure

Abstract

Using atomistic simulations, we have studied the effects of uniaxial load on phase separation in a binary alloy with face-centered cubic structure. The two kinds of atoms have different radii and there is a harmonic coupling between nearest neighbour atoms. Integrating out the vibrational degrees of freedom induces long range elastic interactions. Quenching the system into the miscibility gap from a high temperature initial state, the system's behavior depends strongly on the applied external stress. Without external stress the composition modulations along the elastically soft ⟨100⟩ directions lead to a nearly periodic arrangement of solute precipitates. A uniaxial external stress applied along the [100] direction induces a planar morphology perpendicular to the stress direction in the case of a compressive stress, whereas needle-like precipitates are formed along the stress direction in the case of a tensile stress.

Introduction

The close connection between the microstructure of an alloy and its macroscopic properties is the reason for the great interest in the shape and arrangement of precipitates. An important example is the phenomenon of directional coarsening or rafting, when certain alloys containing misfitting precipitates are subjected to an external load. Depending on whether the external stress is compressive or tensile, the microstructures that develop are completely different, either needle-like or plate-like. Different theoretical approaches have been pursued to model the kinetics of this process, including sharp and diffuse interface models, as well as atomistic simulations [1]. The latter approach was quite successful in predicting the breaking of the cubic symmetry of the alloy due to external stress. In 2-dimensional simulations, the kinetics of formation of stripe-like structures was studied in detail [2,3]. The obvious shortcoming of such 2-dimensional simulations is that needle-like and plate-like domain morphologies cannot be distinguished, since they both appear as stripes in two dimensions. Here we present the first results using a 3-dimensional model crystal with face-centered cubic structure.

Model and Simulations

Our microscopic model is an extension of a conceptually simple 2-dimensional elastically anisotropic model of a binary alloy [1,2] to three dimensions. We consider a fcc lattice $\mathcal{L}$ with L cubic cells in each direction, containing $N = 4L^3$ sites, and periodic boundary conditions. N_A atoms of type A with radii R_A and N_B atoms of type B with radii $R_B < R_A$ are placed near each site $\mathbf{p}\epsilon\mathcal{L}$. A spin variable $\gamma(\mathbf{p})$ is assigned at each $\mathbf{p}\epsilon\mathcal{L}$, with $\gamma(\mathbf{p}) = 1$ if there is an A atom at site $\mathbf{p}$ and $\gamma(\mathbf{p}) = -1$ if there is a B atom there. To model the elastic interactions, all nearest-neighbor pairs of atoms are considered to be connected by springs

with a longitudinal and two different transverse spring constants. The three independent macroscopic elastic constants of a cubic crystal are then given by the long-wave relations[4].

Under the assumption that the atoms come to thermal equilibrium much faster than they diffuse to a new position on the lattice, an effective Hamiltonian for the system can be written in Fourier space as [4,5],

$$\mathcal{H} = \frac{1}{2} \sum_{\mathbf{k}} \Phi(\mathbf{k}) \mid \tilde{\gamma}(\mathbf{k}) \mid^2 \tag{1}$$

where $\tilde{\gamma}(\mathbf{k})$ denotes the Fourier transform of the spin variable $\gamma(\mathbf{p})$. $\Phi(\mathbf{k})$ depends on the length *and* the direction of $\mathbf{k}$ and includes both a short-range chemical interaction (which is chosen to be attractive between the atoms leading to phase separation) and a long-range elastic interaction. In the case of an additional external stress applied on the system, a weak dependence of the elastic constants (i.e. the spring constants) on the local composition has to be considered in order to observe non-trivial effects. Assuming the external stress to be large enough to cause displacements of the atoms from their reference sites which are much larger than their displacement due to the elastic forces, the Hamiltonian can again be written in the form of Eq.(1) [3]. The algorithm in our simulations , in essence, amounts to the Metropolis algorithm with Kawasaki exchange dynamics. The time unit in the simulations is one Monte Carlo step (MCS), i.e. one attempted update of every lattice site. Although a special updating procedure described in [2] was used to deal with the long-range interaction potential, the simulations proved to be time-consuming even on modern workstations and supercomputers.

The numerical values chosen for the spring constants correspond to the experimentally obtained Born-von Karman parameters of copper resulting in a negative elastic anisotropy. A lattice misfit between a pure A phase and a pure B phase of about 4% was assumed. The results presented here were performed on a lattice with $L = 48$, i.e. $N = 442368$ lattice sites, at a temperature $T = 0.51T_0$, T_0 being the critical temperature of an nearest-neighbor Ising model on a fcc lattice. The concentration of the A atoms was $c_A = N_A/N = 0.2$.

Results

The three columns of Figure 1 summarize the evaluation of the end configurations obtained after 1000 MCS with our MC simulations. Each column corresponds to a different stress case described at the top of the figure. Arrows or circular symbols (in the case that the direction of stress is the line of vision) mark the direction of the applied stress. To reduce the 3-dimensional configuration of atoms to a 2-dimensional plot, we averaged the concentration normal to the stress-direction in the first row ((i)-(iii)), and along the stress-direction in the second row ((iv)-(vi)). Bright (dark) regions indicate a high (low) intensity of solute A atoms. The six plots above the bar can be read like "X-ray transmission micrographs", assuming that only one of the phases is absorbant for X-rays.

In the case of no applied stress, the top view (i) and the side view (iv) of the specimen are similar. The precipitates form at equal distances along the elastically soft $\langle 100 \rangle$ directions forming a nearly periodic arrangement. This symmetry between the $\langle 100 \rangle$ directions is broken for the case of an applied external stress as can be easily observed by comparing the corresponding plots in row 1 and 2 ((ii) and (v), (iii) and (vi)). The plots (ii) and (iii), top views of the specimens with tensile and compressive stress, respectively, show a striped structure rotated 90° with respect to each other. This is the result already known from 2-d simulations [3]. The difference of the three-dimensional case becomes apparent in the side view along the stress direction: for the tensile case (v) bright spots are visible indication that the stripes are really needles. Conversely, the side view in the compressive case (vi) reveals no obvious details: in accordance with experiments, the A atoms cluster in plate-like structures

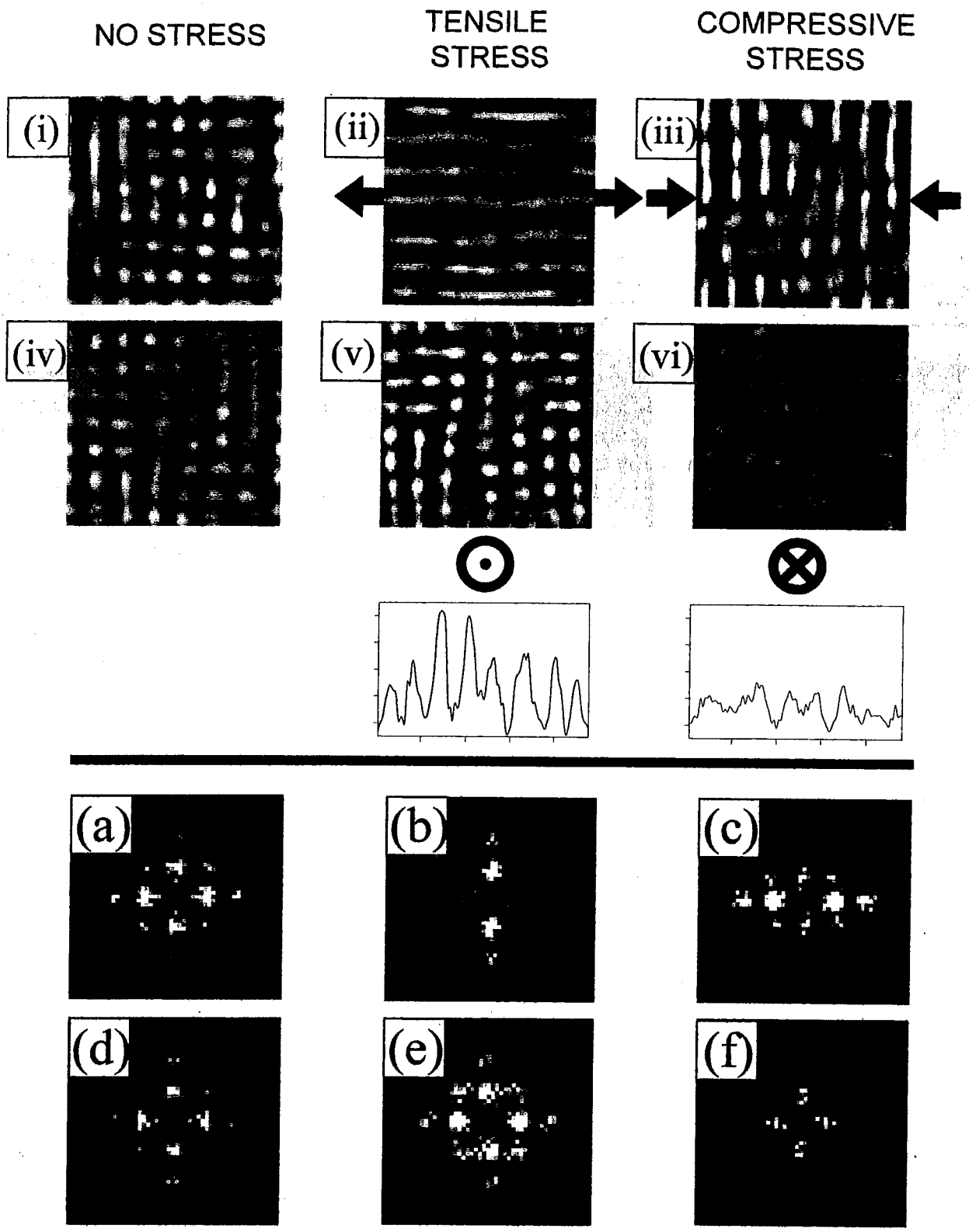

Figure 1: The concentration after 1000 MCS averaged normal to ((i)-(iii)) and along ((iv)-(vi)) the stress direction for the case of zero ((i), (iv)), tensile ((ii), (v)) and compressive ((iii), (vi)) external stress is shown in the first two rows. The third row shows 1-dimensional plots of the average concentration in a direction normal to the external stress, for tensile and compressive stress. In the last two rows sections through the 3-dimensional structure function S(**k**) along the (001) plane ((a)-(c)) and along the (100) plane ((d)-(f)) are plotted for the three different stress cases.

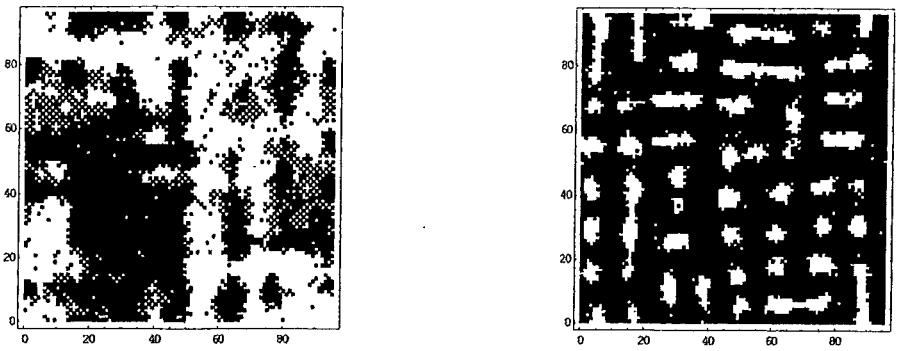

Figure 2: Compressive (left) and tensile (right) configurations after 1000 MCS, viewed along the direction of external stress. Two adjacent (100) planes from the fcc lattice are superposed to form a simple square lattice of lattice parameter $a/2$. In the compressive case a "double-plane" with a maximal number of white A atoms is shown.

perpendicular to the stress direction. The texture visible in (vi) indicates that the plates have thickness variations that are somewhat reminiscent of the structures visible in (iv) or (v). To highlight the difference between (v) and (vi), we have also drawn 1-dimensional concentration plots along directions perpendicular to the external stress. The concentration modulations are much smaller in (vi) than (v). Instead of averaging, we have also plotted a typical (100) plane perpendicular to the stress direction (Fig. 2), for the compressive case (left) and the tensile case (right). The right picture is clearly a section through an array of parallel needles perpendicular to the plane of section. The left image, however, reveals some new details: in fact, the (whitish) plate-like structure has holes in it, which may explain the texture seen in the averaged picture (vi).

Sections through the 3-dimensional structure function $S(\mathbf{k})$ (i.e., the squared Fourier transform of the configuration, $S(\mathbf{k}) = \mid \sum_{\mathbf{p}} e^{i\mathbf{k}\cdot\mathbf{p}} \gamma(\mathbf{p}) \mid^2$) are shown below the bar in Fig. 1. The six plots show the section along the (001) plane ((a)-(c)) and along the (100) plane ((d)-(f)), where the external stress was applied along the [100] direction. They correspond to measurements of the small-angle scattering of X-rays or neutrons using single crystals. Again there is hardly any difference between (a) and (d) in the no-stress case. The striped configurations of (ii) and (iii) translated into Fourier space ((b) and (c)) appear as a nearly 1-dimensional series of peaks. For the tensile case (e) the scattering pattern corresponds to the regular array of needles, whereas for the tensile case (f) the regularity of the arrangement of the precipitates in a plane rectangular to the stress direction seems rather poor. The main maxima of $S(\mathbf{k})$ at $k \approx \frac{2\pi}{La}8$ correspond to a spacing in the crystal of about $6a$, a the lattice parameter. This is exactly the spacing between precipitates in the no-stress case and between needles in the tensile and plates in the compressive case. Maxima of higher order, best observable in plot (e), indicate a high regularity in the arrangement of the precipitates.

References

[1] For a recent overview see: P. Fratzl, O. Penrose and J.L. Lebowitz, *J. Stat. Phys.*, in print.

[2] P. Fratzl and O. Penrose, *Acta metall. mater.* **43**, 2921, (1995); P. Fratzl and O. Penrose, *Acta mater.* **44**, 3227 (1996).

[3] C.A. Laberge, P. Fratzl and J.L. Lebowitz, *Phys. Rev. Lett.* **75**, 4448, (1995); C.A. Laberge, P. Fratzl and J.L. Lebowitz, *Acta mater.* **45**, 3949, (1997).

[4] H.E. Cook and D. DeFontaine, *Acta metall.* **17**, 915 (1969).

[5] A.G. Khachaturyan, *Soviet Phys. Crystallogr.* **10**, 248 (1965).